AFRL-AFOSR-VA-TR-2023-0384

Iron Fiber Laser

Schepler, Kenneth
UNIVERSITY OF CENTRAL FLORIDA
4000 CNTRL FLORIDA BLVD
ORLANDO, FL,
US

07/06/2023
Final Technical Report

Air Force Research Laboratory
Air Force Office of Scientific Research
Arlington, Virginia 22203
Air Force Materiel Command

REPORT DOCUMENTATION PAGE

PLEASE DO NOT RETURN YOUR FORM TO THE ABOVE ORGANIZATION.

1. REPORT DATE	2. REPORT TYPE	3. DATES COVERED	
20230706	Final	START DATE 20190415	END DATE 20230414

4. TITLE AND SUBTITLE
Iron Fiber Laser

5a. CONTRACT NUMBER	5b. GRANT NUMBER	5c. PROGRAM ELEMENT NUMBER
	FA9550-19-1-0127	61102F

5d. PROJECT NUMBER	5e. TASK NUMBER	5f. WORK UNIT NUMBER

6. AUTHOR(S)
Kenneth Schepler

7. PERFORMING ORGANIZATION NAME(S) AND ADDRESS(ES)
UNIVERSITY OF CENTRAL FLORIDA
4000 CNTRL FLORIDA BLVD
ORLANDO, FL
US

8. PERFORMING ORGANIZATION REPORT NUMBER

9. SPONSORING/MONITORING AGENCY NAME(S) AND ADDRESS(ES)	10. SPONSOR/MONITOR'S ACRONYM(S)	11. SPONSOR/MONITOR'S REPORT NUMBER(S)
Air Force Office of Scientific Research 875 N. Randolph St. Room 3112 Arlington, VA 22203	AFRL/AFOSR RTB1	AFRL-AFOSR-VA-TR-2023-0384

12. DISTRIBUTION/AVAILABILITY STATEMENT
A Distribution Unlimited: PB Public Release

13. SUPPLEMENTARY NOTES

14. ABSTRACT
Transition metal (TM) ions doped into chalcogenide crystals have been developed into commercially available mid-infrared (MIR) laser systems. However, these crystalline laser materials are not amenable to drawing into fiber. Here we report on the development of an optically active composite material consisting of Fe-doped ZnSe microparticles suspended in a chalcogenide glass matrix. This is a promising class of solid-state materials which can be drawn into a new generation of optical fibers for efficient and broadly tunable mid-infrared (MIR) lasers. A base chalcogenide glass (94.6% As2S3 5.4% As2Se3) was fabricated and shown to provide good refractive index matching in the 3-5 µm region, necessary to reduce scattering by the ZnSe particles, However, powders of the base glass and ZnSe when mixed and heated to form a composite material showed signs of ZnSe being converted to ZnS. To address this issue, Fe2+:ZnSe particles were coated with a conformal shell of Al2O3, via Atomic Layer Deposition (ALD) to improve the stability of the Fe2+:ZnSe particles in the chalcogenide glass matrix melt environment. An ozone pretreatment of the ZnSe powders prior to ALD also improved particle stability, resulting in significant reduction in dissolution of coated powders. Moreover, an improvement in the drying protocol of the glass resulted in significantly lower impurity concentrations. Optical activity of the Fe2+ ions after fabrication of the composite material was confirmed by measuring broadband optical emission in the 3.52-5.20 µm region when pumped at 2.9 µm using an Er3+:YAG laser. Recent improvements in ALD coating and drying protocols resulted in a bulk optical composite with higher emission signal compared to previous composite material fabricated without these protocols, for the same loading levels. Preforms of the improved composites were drawn into fibers ~250 µm in diameter. However, issues with particle agglomeration in the composite material and bubble formation resulted in high scattering losses and remain to be addressed.

15. SUBJECT TERMS

16. SECURITY CLASSIFICATION OF:			17. LIMITATION OF ABSTRACT	18. NUMBER OF PAGES
a. REPORT U	b. ABSTRACT U	c. THIS PAGE U	UU	21

19a. NAME OF RESPONSIBLE PERSON	19b. PHONE NUMBER *(Include area code)*
JOHN LUGINSLAND	000-0000

Standard Form 298 (Rev.5/2020)
Prescribed by ANSI Std. Z39.18

REPORT DOCUMENTATION PAGE

1. REPORT DATE	2. REPORT TYPE	3. DATES COVERED	
		START DATE	END DATE
27 June 2023	Final	15 April 2019	14 April 2023

4. TITLE AND SUBTITLE

Iron Fiber Laser

5a. CONTRACT NUMBER	5b. GRANT NUMBER	5c. PROGRAM ELEMENT NUMBER
FA9550-19-1-0127		
5d. PROJECT NUMBER	**5e. TASK NUMBER**	**5f. WORK UNIT NUMBER**

6. AUTHOR(S)

Kenneth L. Schepler, Kathleen A. Richardson and Martin C. Richardson

7. PERFORMING ORGANIZATION NAME(S) AND ADDRESS(ES)

UNIVERSITY OF CENTRAL FLORIDA BOARD OF TRUSTEES,
THE OFFICE OF RESEARCH
4000 CENTRAL FLORIDA BLVD
ORLANDO FL 32816-8005

8. PERFORMING ORGANIZATION REPORT NUMBER

9. SPONSORING/MONITORING AGENCY NAME(S) AND ADDRESS(ES)

USAF, AFRL DUNS 143574726
AF OFFICE OF SCIENTIFIC RESEARCH
875 NORTH RANDOLPH STREET, RM 3112
ARLINGTON VA 22203-1954

10. SPONSOR/MONITOR'S ACRONYM(S)

AFOSR

11. SPONSOR/MONITOR'S REPORT NUMBER(S)

12. DISTRIBUTION/AVAILABILITY STATEMENT

DISTRIBUTION STATEMENT A. Approved for public release: distribution unlimited.

13. SUPPLEMENTARY NOTES

14. ABSTRACT

Transition metal (TM) ions doped into chalcogenide crystals have been developed into commercially available mid-infrared (MIR) laser systems. However, these crystalline laser materials are not amenable to drawing into fiber. Here we report on the development of an optically active composite material consisting of Fe-doped ZnSe microparticles suspended in a chalcogenide glass matrix. This is a promising class of solid-state materials which can be drawn into a new generation of optical fibers for efficient and broadly tunable mid-infrared (MIR) lasers. A base chalcogenide glass (94.6 As2S3, 5.4 As2Se3) was fabricated and shown to provide good refractive index matching in the 3-5 μm region, necessary to reduce scattering by the ZnSe particles, However, powders of the base glass and ZnSe when mixed and heated to form a composite material showed signs of ZnSe being converted to ZnS. To address this issue, Fe2+:ZnSe particles were coated with a conformal shell of Al2O3, via Atomic Layer Deposition (ALD) to improve the stability of the Fe2+:ZnSe particles in the chalcogenide glass matrix melt environment. An ozone pretreatment of the ZnSe powders prior to ALD also improved particle stability, resulting in significant reduction in dissolution of coated powders. Moreover, an improvement in the drying protocol of the glass resulted in significantly lower impurity concentrations. Optical activity of the Fe2+ ions after fabrication of the composite material was confirmed by measuring broadband optical emission in the 3.52-5.20 μm region when pumped at 2.9 μm using an Er3+:YAG laser. Recent improvements in ALD coating and drying protocols resulted in a bulk optical composite with higher emission signal compared to previous composite material fabricated without these protocols, for the same loading levels. Preforms of the improved composites were drawn into fibers ~250 μm in diameter. However, issues with particle agglomeration in the composite material and bubble formation resulted in high scattering losses and remain to be addressed.

15. SUBJECT TERMS
infrared, laser, chalcogenide, fiber, transition metal, iron, Atomic Layer Deposition

16. SECURITY CLASSIFICATION OF:			17. LIMITATION OF ABSTRACT	18. NUMBER OF PAGES
a. REPORT	b. ABSTRACT	C. THIS PAGE		
U	U	U	SAR	19

19a. NAME OF RESPONSIBLE PERSON	19b. PHONE NUMBER *(Include area code)*
Kenneth L Schepler	407-823-6830

INSTRUCTIONS FOR COMPLETING SF 298

1. REPORT DATE.
Full publication date, including day, month, if available. Must cite at least the year and be Year 2000 compliant, e.g. 30-06-1998; xx-06-1998; xx-xx-1998.

2. REPORT TYPE.
State the type of report, such as final, technical, interim, memorandum, master's thesis, progress, quarterly, research, special, group study, etc.

3. DATES COVERED.
Indicate the time during which the work was performed and the report was written.

4. TITLE.
Enter title and subtitle with volume number and part number, if applicable. On classified documents, enter the title classification in parentheses.

5a. CONTRACT NUMBER.
Enter all contract numbers as they appear in the report, e.g. F33615-86-C-5169.

5b. GRANT NUMBER.
Enter all grant numbers as they appear in the report, e.g. AFOSR-82-1234.

5c. PROGRAM ELEMENT NUMBER.
Enter all program element numbers as they appear in the report, e.g. 61101A.

5d. PROJECT NUMBER.
Enter all project numbers as they appear in the report, e.g. 1F665702D1257; ILIR.

5e. TASK NUMBER. Enter all task numbers as they appear in the report, e.g. 05; RF0330201; T4112.

5f. WORK UNIT NUMBER.
Enter all work unit numbers as they appear in the report, e.g. 001; AFAPL30480105.

6. AUTHOR(S). Enter name(s) of person(s) responsible for writing the report, performing the research, or credited with the content of the report. The form of entry is the last name, first name, middle initial, and additional qualifiers separated by commas, e.g. Smith, Richard, J, Jr.

7. PERFORMING ORGANIZATION NAME(S) AND ADDRESS(ES). Self-explanatory.

8. PERFORMING ORGANIZATION REPORT NUMBER.
Enter all unique alphanumeric report numbers assigned by the performing organization, e.g. BRL-1234; AFWL-TR-85-4017-Vol-21-PT-2.

9. SPONSORING/MONITORING AGENCY NAME(S) AND ADDRESS(ES). Enter the name and address of the organization(s) financially responsible for and monitoring the work.

10. SPONSOR/MONITOR'S ACRONYM(S). Enter, if available, e.g. BRL, ARDEC, NADC.

11. SPONSOR/MONITOR'S REPORT NUMBER(S). Enter report number as assigned by the sponsoring/monitoring agency, if available, e.g. BRL-TR-829; -215.

12. DISTRIBUTION/AVAILABILITY STATEMENT. Use agency-mandated availability statements to indicate the public availability or distribution limitations of the report. If additional limitations/ restrictions or special markings are indicated, follow agency authorization procedures, e.g. RD/ FRD, PROPIN, ITAR, etc. Include copyright information.

13. SUPPLEMENTARY NOTES. Enter information not included elsewhere such as: prepared in cooperation with; translation of; report supersedes; old edition number, etc.

14. ABSTRACT. A brief (approximately 200 words) factual summary of the most significant information.

15. SUBJECT TERMS. Key words or phrases identifying major concepts in the report.

16. SECURITY CLASSIFICATION. Enter security classification in accordance with security classification regulations, e.g. U, C, S, etc. If this form contains classified information, stamp classification level on the top and bottom of this page.

17. LIMITATION OF ABSTRACT. This block must be completed to assign a distribution limitation to the abstract. Enter UU (Unclassified Unlimited) or SAR (Same as Report). An entry in this block is necessary if the abstract is to be limited.

Final Report
AFOSR Grant FA9550-19-1-0127
Title: Iron Fiber Laser

Institution Proposal Number: 1066190

Principal Investigator:

Kenneth L Schepler, PhD
CREOL, The College of Optics & Photonics
University of Central Florida
4304 Scorpius St
Orlando, FL 32816-2700
407-823-6830 schepler@creol.ucf.edu

CoPIs: Kathleen Richardson and Martin Richardson

Start Date: **15 April 2019**
End Date: **14 April 2023**

Table of Contents

Metrics (bottom line up front)

Statement of Work Tasks and Accomplishments

1. Fabricate a mid-IR broadly tunable nanocomposite laser material consisting of Fe^{2+} doped ZnSe particles in a chalcogenide glass matrix with low scattering loss and Fe^{2+} emission/absorption of bulk Fe:ZnSe.

Initial samples of chalcogenide glass doped with Fe:ZnSe particles were fabricated but showed no sign of Fe^{2+} optical activity. X-ray measurements showed that ZnSe particles did *not* remain after incorporation into the chalcogenide glass matrix but ZnS crystal patterns were observed. Atomic layer deposition (ALD) of a shell of alumina (Al_2O_3) around the ZnSe particles was found to prevent dissolution into the chalcogenide glass matrix during heating. X-ray measurements also showed that ZnSe particles did remain after incorporation into the chalcogenide glass matrix. Improvements towards complete and uniform shell coating were achieved. ALD process changes reduced the tendency of ZnSe particles to agglomerate.

2. Investigate physical and optical characteristics of Fe ions in ZnSe related to changes in particle size and size distribution and particle surface functionality, particularly where surface states and quantum confinement could be important.

Alumina-coated Fe:ZnSe particles suspended in a chalcogenide glass matrix were investigated for optical activity. Spectra of Fe^{2+} emission when optically pumped at 3 μm were observed proving that alumina-coated Fe:ZnSe particles do not dissolve during the heating needed to incorporate the particles in a chalcogenide glass matrix.

3. Demonstrate lasing in a Fe:ZnSe/chalcogenide nanocomposite bulk sample.

This task was put on hold until Fe^{2+} emission could be demonstrated in a ZnSe particle-chalcogenide glass matrix. Sample materials produced up to this point had optical emission but large losses.

4. Fabricate Fe:ZnSe/chalcogenide nanocomposite in fiber form while maintaining the Fe^{2+} emission and absorption properties of bulk Fe:ZnSe.

Fabrication of composite chalcogenide fiber containing coated ZnSe particles was achieved although clumps were present throughout the fiber length due to agglomeration of particles prior to the fiber draw. Recent improvements in powder coating protocols reduced particle agglomeration. Preforms containing ZnSe (both ZnSe powder and Fe-doped microcrystallites) were drawn into fiber at the University of Nottingham. However optical loss was high due to bubbles, agglomeration and impurities found in the base glass.

5. Demonstrate multi-watt Fe lasing of Fe:ZnSe/chalcogenide nanocomposite in fiber form.

Attempts to observe Fe^{2+} optical activity in the matrix fibers were unsuccessful. Passive losses due to bubbles, agglomerates and impurities need to be reduced before lasing can be achieved.

Statement of Objectives

The objective of this effort was to demonstrate a high-power fiber laser that is wavelength tunable in the 4-5 μm part of the infrared spectrum. Mid-infrared light is of interest for numerous applications including medical imaging and diagnostics, remote sensing of chemicals, and infrared countermeasures against heat-seeking missiles. The proposed fiber laser form is often preferred for practical applications such as its flexibility, insensitivity to vibrations and excellent thermal management. Fe^{2+}-doped ZnSe wwas used as the active lasing material in this effort. However, since ZnSe is a crystalline material, it is not amenable to fabrication in fiber form. Instead, we proposed fabricating a laser material composite consisting of Fe^{2+}

doped ZnSe micro-particles suspended in a chalcogenide glass matrix (Figure 1)). Optical activity was characterized and preforms of the composite material with good performance were drawn into fiber. Optical absorption and emission properties (Figure 2) were then investigated with the ultimate objective of high-power lasing.

We know that pure chalcogenide glass can be drawn into fiber form as evidenced by commercial sales of such fibers. Powers > 10 W have been delivered through single-mode chalcogenide fiber [1]. Suspending Fe:ZnSe particles in the glass matrix required fabrication of chalcogenide glass (ChG) with a refractive index that matches ZnSe to prevent scattering loss. Fabrication of the mixture required grinding the ChG and the Fe:ZnSe into power and then remelting the mixture (actually, just the glass) to form a composite of Fe:ZnSe particles in the ChG. Of course, the Fe^{2+} ions must remain intact in the ZnSe particles and achieving that became a major part of our research effort.

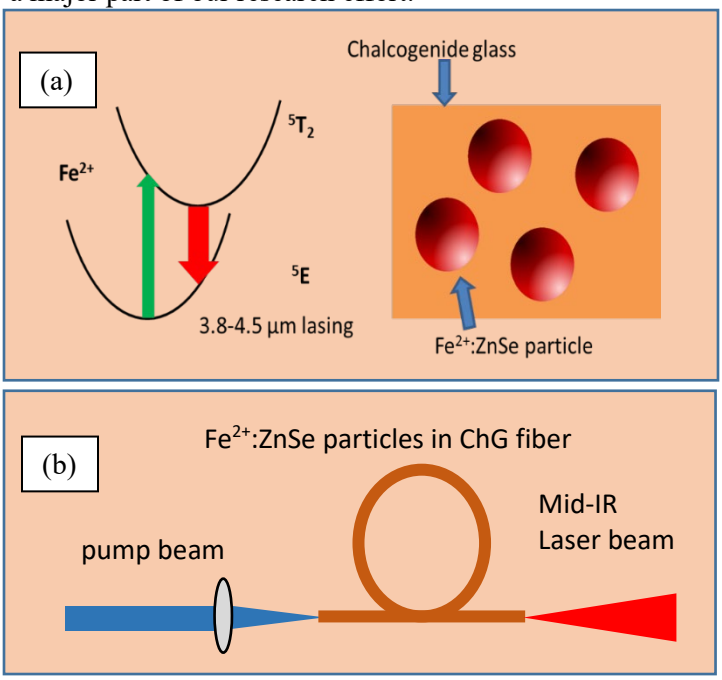

Figure 1 (a) Energy levels of Fe^{2+} ions in a ZnSe crystal where Fe^{2+} ions substitute for Zn^{2+} ions and schematic of the concept of Fe:ZnSe particles immersed in a chalcogenide glass matrix. (b) Concept of an optically pumped iron fiber laser.

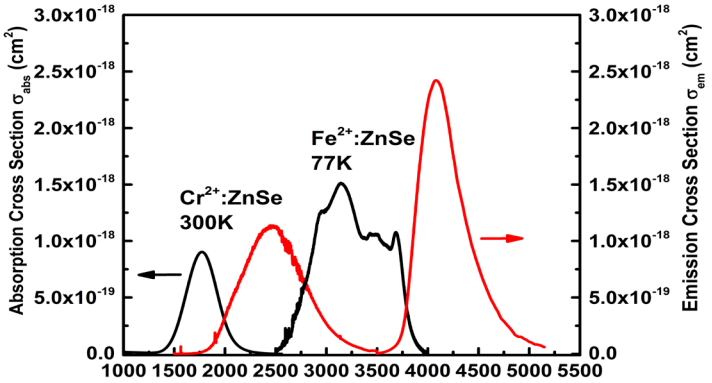

Figure 2. Cr^{2+} and Fe^{2+} emission and absorption properties.

Finally, we planned to demonstrate multi-Watt Fe lasing of Fe:ZnSe/chalcogenide nanocomposite in fiber form. No Fe fiber lasers operating in the 4-5 μm region have been previously demonstrated and other fiber lasers (rare-earth ion doped glasses) are limited to very low powers. Based upon preliminary investigations reviewed below we assumed material fabrication for the iron fiber laser effort would be straightforward. But *nature* had some tricks up her sleeve that captured our attention.

Preliminary Cr:ZnSe in ChG Investigations

In our preliminary work prior to grant award, composite materials made of Cr^{2+}:ZnSe micro-crystals embedded in As_2S_3/As_2Se_3 glass were prepared. The synthesis route used was the so-called grinding re-melt technique where the composites are made by grinding an initial base glass and mixing in Cr^{2+}:ZnSe crystal powder before re-melt. The synthesis (melting) was made at 800˚C, far below the ZnSe melting point of 1525ºC. It is possible to get homogeneous materials by this way, thanks to the high synthesis temperature. Crystalline particles were observed via white-light interferometry and SEM measurements of sample surfaces after etching. However, the IR absorption characterization of the resulting material did not reveal the expected presence of a Cr^{2+} absorption peak in the 1.8 μm region. We speculated that our small samples had loading fractions of Cr^{2+}:ZnSe particles too low for easy detection. Or perhaps the Cr^{2+} ions were diffusing out of the ZnSe particles into the glass matrix at the melt temperature used for the synthesis (800˚C). We expected reductions in time and temperature for the remelt step as well as increased loading of iron or chromium-doped ZnSe particles would solve the problem. Subsequent efforts in our multi-year effort aimed to answer these questions.

Identifying the Problem

During the first two years of our effort, we discovered that the chemistry occurring during the melting of the chalcogenide glass mixed with ZnSe particles was more complex than expected. Details are discussed in our papers published in the Journal of Non-Crystalline Solids. [2, 3] We found that stability of the crystalline dopant within the glass melt was severely impacted by melt conditions. We had developed an optimized chalcogenide glass composition 94.6 As_2S_3 – 5.4 As_2Se_3 designated as base glass (BG); this base glass was designed to be the composite's matrix, tuned to match the refractive index of ZnSe. Very good fiber drawing capability of this glass was demonstrated. But when Fe:ZnSe particles and BG particles, ~25 μm diameter, were mixed and reheated to glass melting temperatures, we could observe microscopic particles present in the glass but could not observe any Fe^{2+} optical activity.

As shown in Figure 3, with increasing temperature and length of time at a given temperature, more and more crystalline ZnS showed up in XRD measurements. Clearly, heating the mixture was causing the ZnSe to dissolve (at least partially) into the BG even though the ZnSe melting point is 1,525ºC, far above the temperatures used. Cooling then resulted in formation of ZnS crystallites since sulfur is the predominant chalcogenide ion in the BG. Iron ions exposed to the glass likely went into the glass matrix resulting in major changes in crystal field and ionization state [4]. Reducing the time and temperature of the remelt lower than those reported in Figure 3 resulted in poor quality composite material with bubbles and cracks.

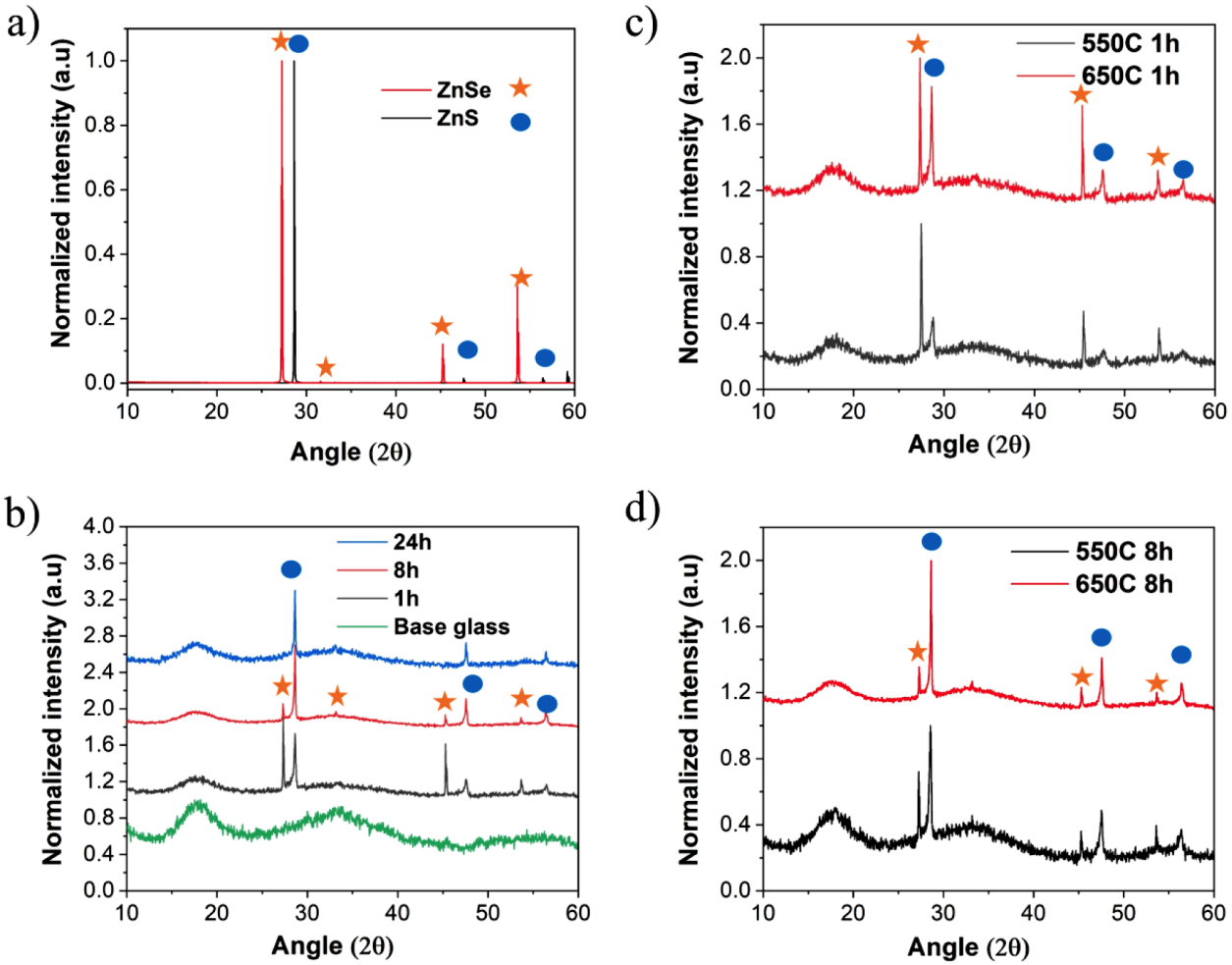

Figure 3. XRD data of (a) ZnSe and ZnS crystals, (b) ZnSe-doped chalcogenide base glass (BG) melted at 650˚C for 1, 8 and 24 hours, (c) ZnSe-doped BG melted at 550 and 650˚C for1 hour and (d) ZnSe doped BG melted at 550 and 650˚C for 8 hours. Diffractograms in (b),(c) and(d) were vertically shifted for clarity.

Preventing dissolution

To prevent dissolution of ZnSe during remelt we sought the help of Prof Banerjee, Materials Science and Engineering UCF. With the help of his group, we investigated the use of a core/shell crystallite design where the ZnSe shell chemistry and morphology attributes were engineered to ensure survivability during the composite material synthesis. The material selected to form the shell was Al_2O_3 due to its stability at BG remelt temperatures and its diffusion barrier characteristics. Alumina shells of ~30 nm thickness were grown on ~25 μm diameter ZnSe particles. A mixture of BG particles and alumina-coated Fe:ZnSe particles (both sieved to ~25 μm diameters) was then heated to form a BG matrix with suspended Fe:ZnSe particles. The entire procedure is portrayed in Figure 4. Composites of BG and alumina-coated ZnSe were examined with X-ray diffraction (XRD) (Figure 5) and showed the presence of both ZnSe and ZnS in samples like that shown in Figure 6. FTIR absorbance spectra of composite samples consisting of ZnSe/Al_2O_3 core/shell particles in BG are shown in Figure 5b. Adding the ZnSe particles significantly increases the baseline loss coefficient. This is likely due to scattering, especially of particle agglomerates. Energy-dispersive X-ray (EDX) spectroscopy (Figure 7) showed that some of the ZnSe particles were only partially coated with the alumina shell. The partial coating may have been due to particle aggregation during the ALD process [3].

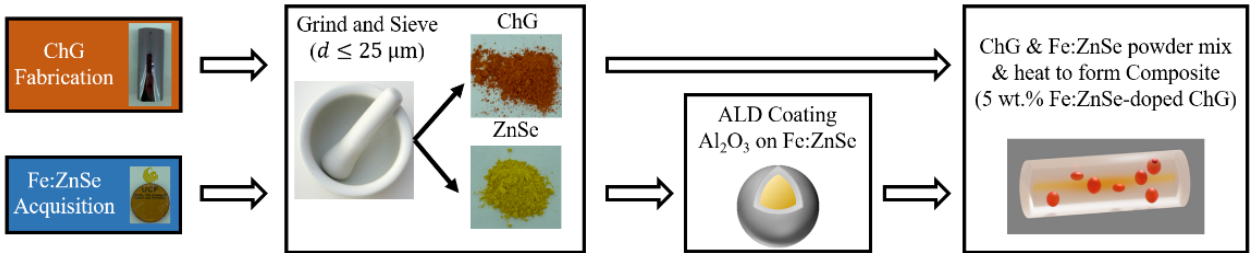

Figure 4. Flow chart describing the synthesis of the Fe:ZnSe-doped ChG composite materials. After fabrication of the ChG and acquisition of the Fe:ZnSe, both materials are ground and sieved to produce microparticles ≤ 25 μm in size. A conformal Al_2O_3 coating is then applied to the Fe:ZnSe powder using atomic layer deposition (ALD). The coated Fe:ZnSe powder is then mixed with the ChG powder at various wt.% loadings before remelting to form a Fe:ZnSe-doped ChG composite material. Pictures of ALD coating and composite material are conceptual.

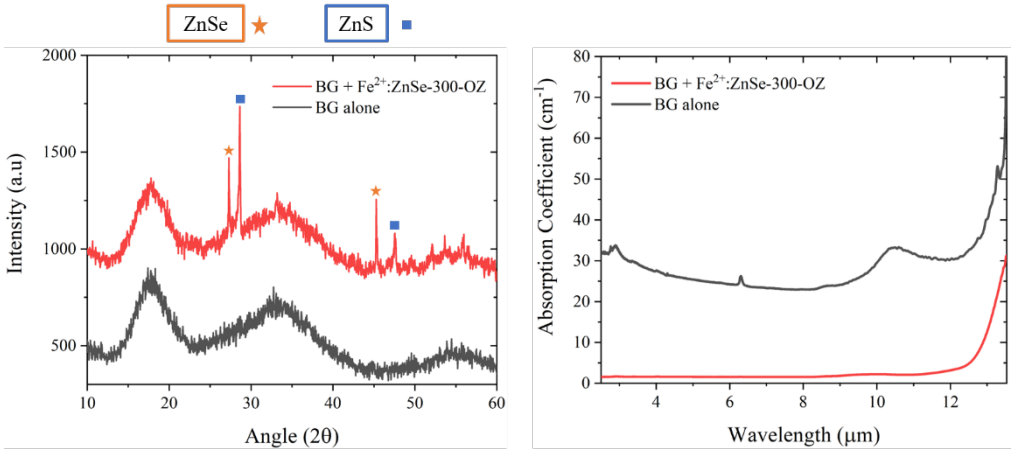

Figure 5. (a) Bulk XRD pattern shows that ZnSe crystallites survived but some ZnS was generated during the remelt process. (b) FTIR shows additional scattering and impurities are introduced when the Fe:ZnSe particles are added and the mixture heated to form the composite.

Figure 6. Composite sample disk of BG with 10% by weight of ZnSe particles coated with ~30 nm of alumina.

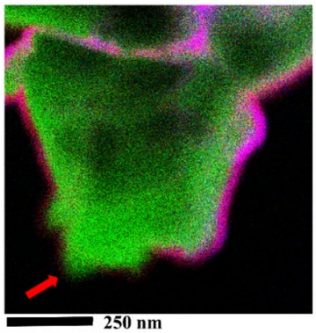

Figure 7. EDX image of a ZnSe particle coated with an alumina shell. The magenta region corresponds to Al + O and the green to Zn +Se. The red arrow points to a surface where the shell may be discontinuous.

Demonstration of Fe^{2+} optical activity

ZnSe particles doped with Fe^{2+} ions were alumina coated via ALD, mixed with BG powder, and run through the remelt process. A sample disk (~1 cm in diameter and 1 mm thick) of the Fe:ZnSe-doped ChG composite (Figure 6) was tested for Fe^{2+} emission using the fluorescence spectroscopy setup shown in Figure 8. The composite material was housed in a liquid nitrogen cooled cryostat outfitted with MgF_2 windows and was held at ~77 K. A flashlamp pumped Er:YAG laser operating in long pulse mode was used to optically excite the composite material. The pump laser output consisted of 49 mJ, 200 µs pulses at 8 Hz repetition rate with a spectrum centered at 2940 nm. Pump light was then focused onto the sample using an off-axis parabolic mirror (f = 20 cm).

The fluorescence emission from the composite material was then collected using a second off-axis parabolic mirror (f = 10 cm) before being imaged onto the entrance slit of a Czerny-Turner monochromator (Horiba Micro-HR, 150 l/mm grating) for spectral analysis. Light transmitted through the monochromator was collected using a 40 mm CaF_2 plano-convex lens and focused onto a mid-IR photodiode (VIGO PVI-5) for signal acquisition. To prevent any spurious signal which may arise from stray pump light, a 3600 nm long pass filter (Edmund Optics #33-970) with a measured attenuation of ~27 dB at the pump wavelength was mounted in front of the photodiode. The photodiode signal was then electronically amplified (34 dB) before being recorded on an oscilloscope.

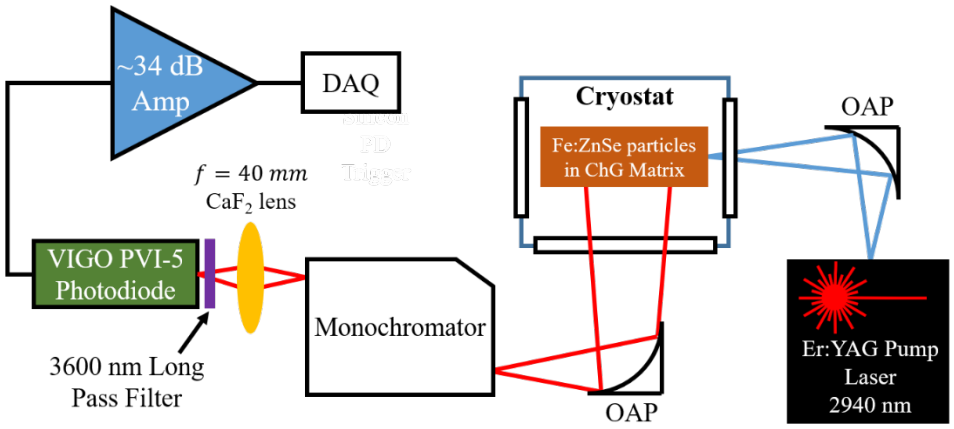

Figure 8. Optical setup used to measure the fluorescence spectrum of 5 wt.% Fe:ZnSe-doped ChG composite material. OAP: off-axis parabolic mirror. DAQ: data acquisition. ChG: chalcogenide glass[5]

A comparison of the Fe^{2+} emission from bulk Fe:ZnSe and Fe:ZnSe particles in the BG ChG matrix is shown in Figure 9. This was our **first** observation of Fe^{2+} optical activity in the composite material. Comparing the composite material data against that obtained from a bulk Fe:ZnSe sample shows a significant peak at 3840 nm in the emission spectrum of the composite sample. The shift from the bulk peak at 4080 nm is similar to the shift of the peak emission wavelength in Fe:ZnS compared to Fe:ZnSe [6]. As indicated in our XRD results, some of the ZnSe particles dissolved or partially dissolved and recrystallized as ZnS. While difficult to verify and quantify, Fe^{2+} ions may be substituting into the ZnS crystals as they crystallize. On the other hand, a shoulder peak at 3840 is also present in the bulk sample. Thus, an alternative explanation could be related to the size of the individual crystallites; near-surface crystal field effects would be stronger in the smaller ZnSe particles present in the composite. Additionally, the expansion coefficient of ZnSe ($7x10^{-6}$ K^{-1}) is one third that of As_2S_3 ($21x10^{-6}$ K^{-1}) so compression of the ZnSe particles during remelt cooling could be increasing the Fe^{2+} crystal field. (personal communication with Sean McDaniel (AFRL/RY)). The explanation for the blue shifted peak needs further investigation. The dip in both the bulk and matrix emission spectra at ~4200 nm is due to absorption by CO_2 in the atmosphere.

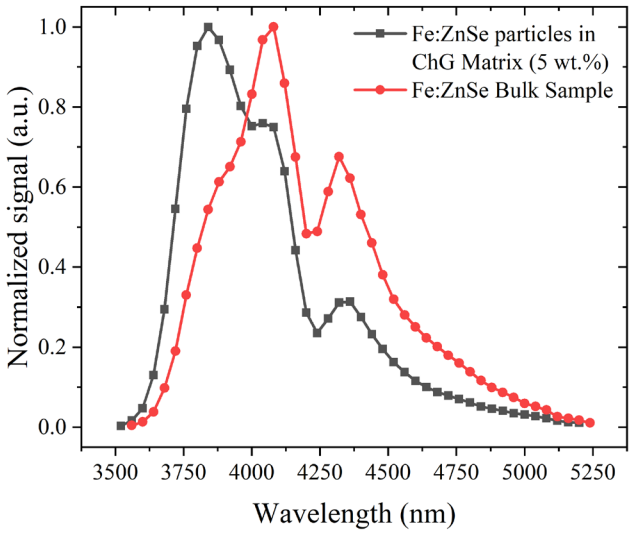

Figure 9. Measured fluorescence spectrum from the 5 wt.% Fe:ZnSe-doped ChG composite (black) and a bulk Fe:ZnSe crystal (red) used as a reference source. [5]

Composite Fiber Drawing

Undoped BG and coated ZnSe matrix fiber

Preforms of BG and coated ZnSe matrix samples were sent to Prof Angela Seddon at the University of Nottingham for fiber drawing experiments. No Fe doping was done to preserve the amount of Fe-doped ZnSe material we have and we expect Fe doping to have no effect on fiber drawing. Figure 10 shows photos of disks taken from the bottom of a composite preform. XRD measurements shown in this figure reveal that ZnSe and ZnS particles are only significantly present in the bottom-most disk. This indicates that particle agglomeration and sedimentation were present as well as partial dissolution of the ZnSe particles. Due to the much higher density of ZnSe (5.2 g/cm^3) compared to As_2S_3 (3.2 g/cm^3) we would expect settling to occur and must devise a method to maintain uniform distribution during cooling.

Fibers were successfully drawn from all 4 preform disks (or bands) shown in Figure 10. Multiple meters of fiber were drawn from each band but lumps appeared every 0.5-0.8 meters (See Figure 11). The lumps are believed to be due to the presence of either ZnSe or ZnS agglomerates or the crystallization of ZnS. Microscopy of the composite fiber is compared to BG fiber in Figure 12. Particles and/or bubbles are observable. Cross sections of the fibers reveal the presence of dark spots that could be due to voids or ZnSe/ZnS crystals. For the moment considering their circular shape, we believe they are more likely holes caused by bubbles formed, due to the ZnSe dissolution during the preform synthesis.

In this effort thus far, we have standardized our efforts to use of ~25 μm BG and ZnSe particles. This produces particles easily observed with optical microscopes and is sufficient for the 250 μm fibers being drawn for this effort. Smaller particles (< 10 μm diameter) will be necessary to draw single-mode fiber but this increases the time and effort to manually grind the powders. However, smaller particles could be more difficult to fabricate, to shell coat, and to prevent aggregation. In addition, as size decreases the relative number of Fe^{2+} ions exposed to surface effects increases.

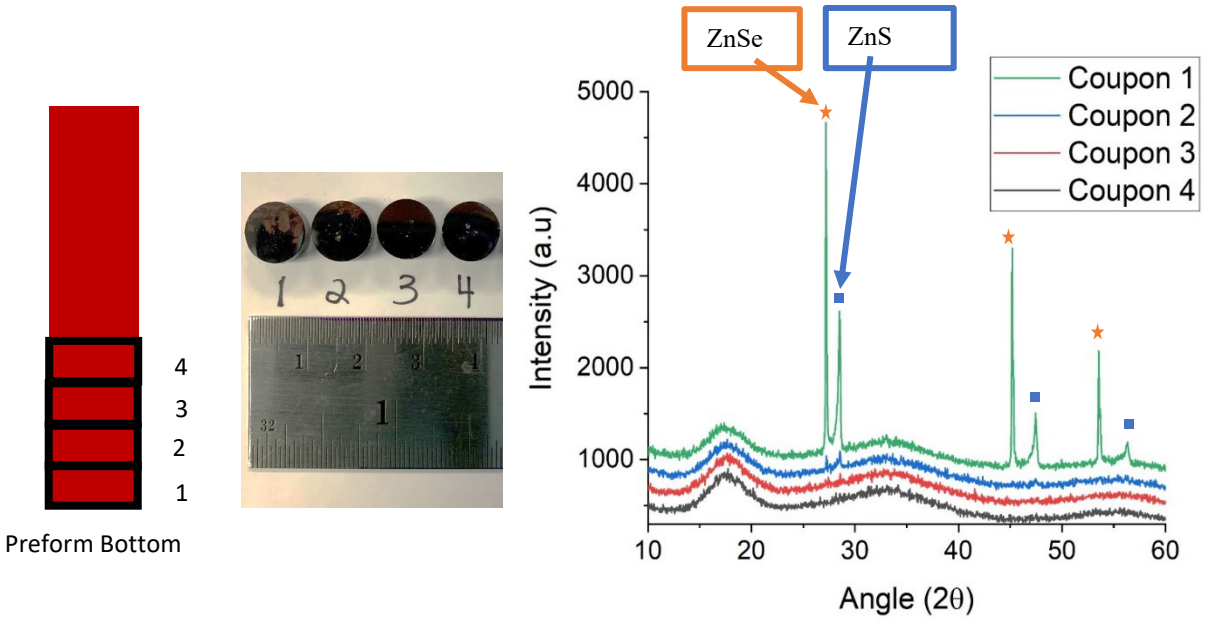

Figure 10. BG + shell-ZnSe preform (1 wt%) sent for fiber draw testing. We note that ZnSe and ZnS were only present in significant amounts in the bottom disk (#1) via XRD measurements.

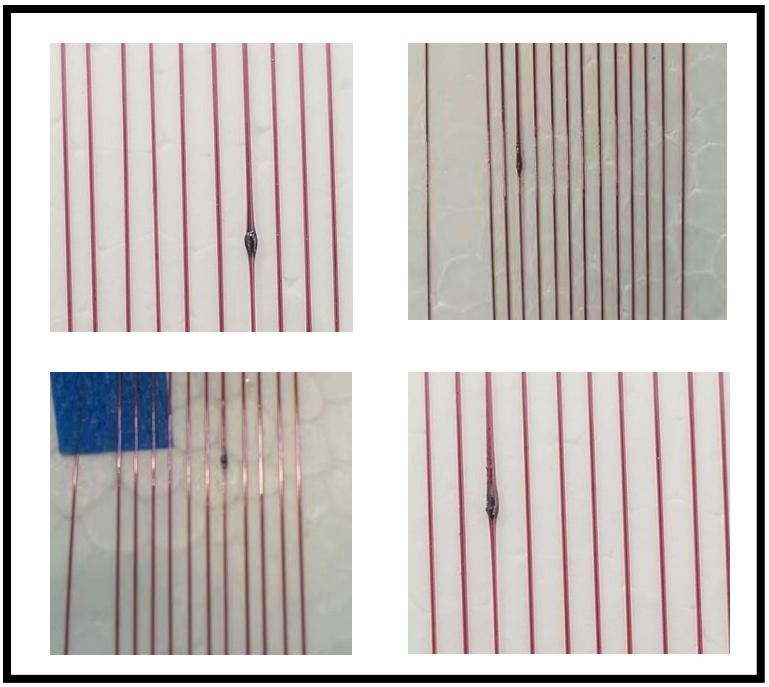

Figure 11. Fibers drawn from composite preforms with 0.5 wt% alumina-coated ZnSe particles. Lumps were observed to occur every 0.5-0.8 m.

Our first ZnSe-doped glass fiber drawing tests showed:

- Regions of good particle dispersion in fiber (below 1 wt% loading)
- Evidence of some particle sedimentation during preform fabrication (reduce T, decrease viscosity)
- Presence of lumps, voids/holes led to scatter loss (but lumps could be cut out)
- Composition and phase of the agglomerates to be determined
- Fiber lengths without lumps to be optically characterized

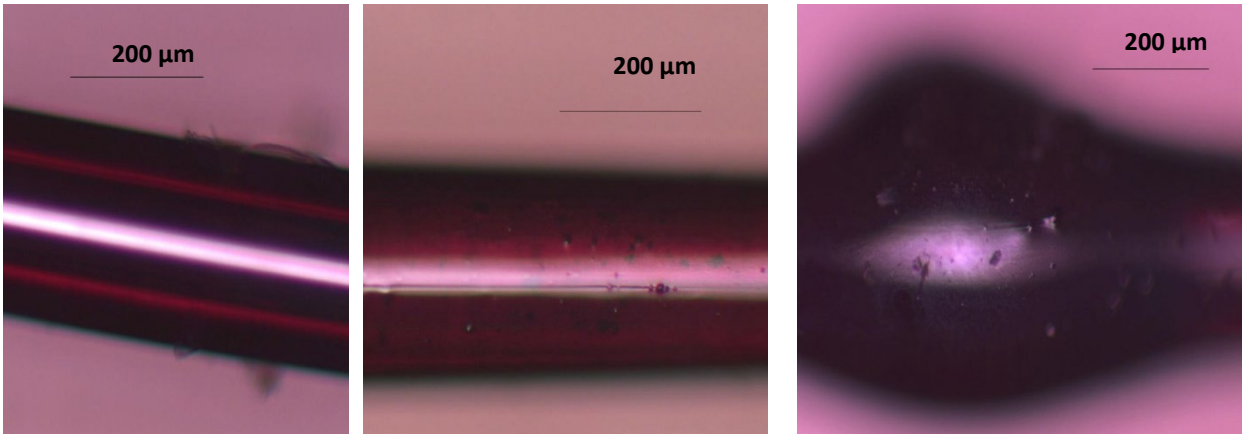

Figure 12. Composite fiber (BG + alumina-shell ZnSe particles) microscopy.

Fe^{2+}-doped matrix improvements

Processes that reduced particle agglomeration and provided improved alumina-coated Fe:ZnSe powder were developed. We improved the quality of ALD alumina shell coating by employing modifications in deposition conditions, as well as controlling the host glass -OH and hydride impurities by raw material purification.

For the ALD process improvement, we added an ozone generator to the ALD furnace (far left of Figure 13). Also in the improved version, the barrel reactor was rotated for even ozone exposure of the Fe:ZnSe powder under controlled environment. The ozone pretreatment was used to oxidize the ZnSe surface. ZnSe is hydrophobic making deposition of Al_2O_3 on ZnSe difficult. Oxidation of the surface makes it hydrophilic allowing Al_2O_3 to be deposited much more easily. The data suggest that a pretreatment of the ZnSe surface with UV-O_3 or the use of a strong oxidant, such as an O_2 plasma during ALD, reduces the incubation delays (cycles of ALD exposure without significant alumina shell growth) and improves growth characteristics of Al_2O_3 on a ZnSe surface. *This was an important modification since it improved the shell coverage of the ZnSe particles and thus reduced the amount of ZnSe converted to ZnS during the powder mixture heating to form composite preforms.*

During mixing of the ChG powder and the Fe:ZnSe powder, the mixture was exposed to atmosphere. To remove moisture accumulated before heating the mixture to glass melting temperatures, we added a drying step. For the improved drying protocol, the glass composite mixture (glass powder and Fe:ZnSe powder) was placed in a 16 mm tube (tube diameter was increased from 14 mm to help bubbles leave the melt before quenching). The tube was then placed in a tube furnace and the powder was dried under dynamic vacuum for 12 hrs. at 150 °C to alleviate moisture related impurities. A reduction in the -OH impurity concentration was shown after the pre-heat treatment process.

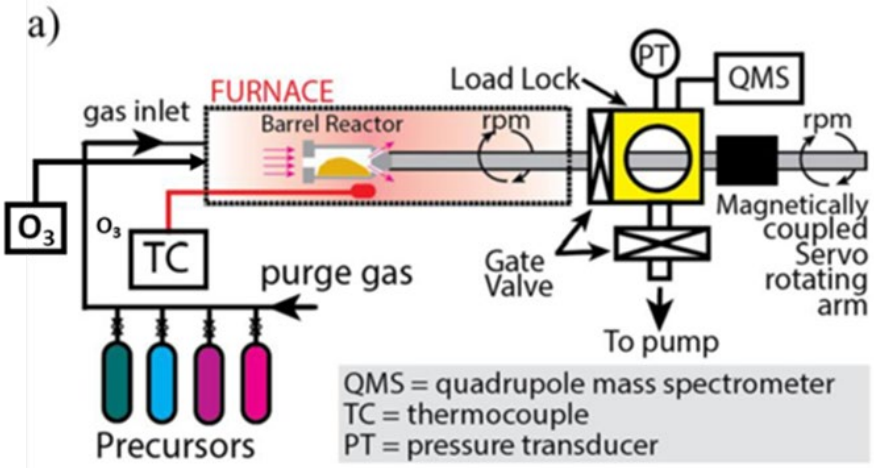

Figure 13. Schematic of ALD furnace.

Aggregates

Aggregates of Fe:ZnSe particles were observed to form in the host glass. The higher dissolution of the ZnSe into the host glass in the highly doped samples (5 wt%) compared to the lower (0.5 and 1.0 wt%) doped composites can be observed in Figure 14. Fe^{2+}:ZnSe tends to settle towards the bottom of the ampoule when the host glass is melted. Maintaining a homogenous distribution of the Fe^{2+}:ZnSe particulates throughout the length of the ampoule has been a challenge in this work. When the Fe^{2+}:ZnSe particles contacted each other, they formed aggregates. These aggregates tended to settle at the bottom of the glass ampoule. As can be seen in Figure 14a, composites with loading 5.0 wt% form aggregates with an average size of 64 (± 5.32) μm observed on the surface of the bottom slice as compared to 28 (± 3.12) μm and 10 (± 1.22) μm for the 1.0 and 0.5 wt% composites respectively. Similarly, aggregates with an average size of 35.32 (± 4.00) μm, 18.16 (± 1.12) μm and 4.05 (± 0.56) μm were observed in the middle slices of the composites from 5 wt%, 1 wt% and 0.5 wt% composites respectively. We note that the aggregate fraction at bottom and middle surfaces scale roughly linearly with ZnSe wt%. Figure 14b shows an SEM image of deposited aggregates on the 5 wt% doped bottom glass slice.

Bubbles

Another observation via SEM image analysis is shown in Figure 14c. The composites had bubbles throughout the volume, the bubbles were circular and deep. EDS analysis to identify chemical composition inside the bubbles was unsuccessful. The bubbles were too deep to focus the electron beam and get elemental composition. The 5 wt% composites had large bubbles ranging from 100 – 300 μm, covering ~ 16% of the sample surface. The low loading composites (1 and 0.5 wt%) samples had 3% and 1.85% of the sample surface was covered with bubbles ranging 40-200 μm. Again, the amount of bubble formation was approximately linearly proportional to the ZnSe loading level. It seems likely that ZnSe particles not completely covered by the alumina shells convert to ZnS when in contact with the base glass and sublimation to gas during the process is forming the bubbles.

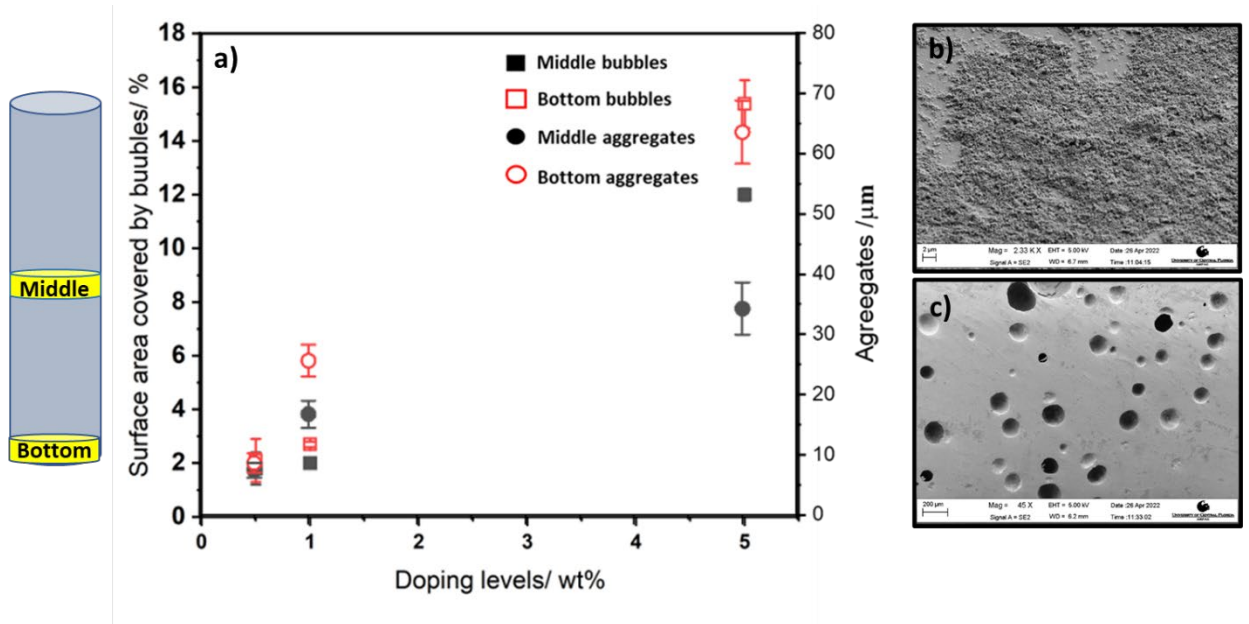

Figure 14. a) Plot showing a comparison between the surface area covered by bubbles and aggregates formed in the Middle and Bottom slices of different loading levels. b) Optical micrograph (scalebar = 2 µm) depicting agglomerates of 64 (± 5.32) µm; c) Optical micrograph of slice taken from the bottom of the 5.0 wt% glass composite showing the large density of bubbles formed by which was believed to be associated with the partial dissolution of ZnSe to form ZnS (scalebar = 200 µm).

Photoluminescent emission

The emission properties of bulk Fe^{2+} doped composites were measured using the experimental setup and protocol discussed previously (Figure 8). The fluorescence signal was measured at ~77 K, both as a function of time and wavelength and compared using a reference Fe^{2+}:ZnSe sample. Figure 15 (left) shows a comparison of the emission signal from two equally doped 5 wt% composites. Despite the composite's loss in the form of impurity absorption and bubble-related scatter loss, broadband emission covering the 3520-5200 nm spectral region was observed, indicating the presence of active Fe^{2+} ions. The new 5 wt% composites made via improved ALD and drying protocol showed higher emission signal with the same loading levels. Figure 15 (right) shows a comparison of the impurity concentrations in the old and new 5 wt% loading level samples. There are high concentrations of -OH and hydride impurities in the old 5 wt% composite. It is also important to understand that there are several factors that impact the emission signal strength including pump beam quality, spot size, layout of the imagining system used to collect the fluorescence signal, and sample orientation. Best efforts were made to maintain the old experimental conditions.

The strong dip in the emission spectrum of both samples around 4.2 µm was due to absorption by atmospheric CO_2. The difference in CO_2 dip between both the samples can be explained via difference in path lengths through the atmosphere. As indicated in the XRD analysis, some of the ZnSe particles dissolved and recrystallized into ZnS. Fe^{2+} ions may be substituting into ZnS crystals, but no spectroscopic evidence of the iron in the glass has been observed.

Despite high scattering loss in the composite material, incorporation of improved ALD coating and purification step (increased drying time) resulted in reduced impurity concentrations which further assisted in observation of higher emission signal making these results promising for future development of fiber laser sources operating at > 4 µm.

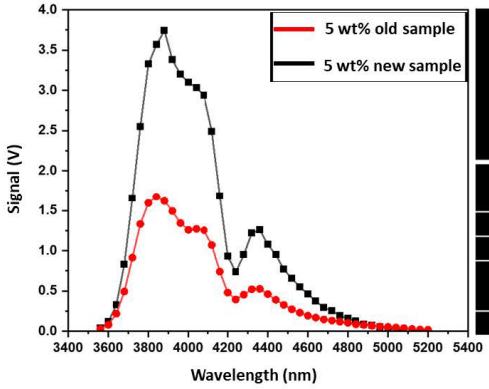

Impurity	Position of the maximum of the absorption band (μm)	Extinction Coefficient, ε (dB/m · ppm)	5.0 wt% (new sample)		5.0 wt% (old sample)	
			α (dB/m)	[Impurity] ppm	α (dB/m)	[Impurity] ppm
H_2O	2.77	-	204	-	456	-
OH	2.90	5.0	310.56	62.22	852.64	170.52
SH	4.02	2.5	64.88	25.95	78.25	31.3
CO_2	4.23	-	44.5	-	52.23	-
Se–H	4.30	1.00	128.38	128.38	156.25	156.25

Figure 15. (left) Shows a comparison of the measured fluorescence spectrum from the 5 wt% Fe^{2+}:ZnSe loaded composites (black) new bulk sample, (red) old equivalently loaded bulk sample, (right) Relevant impurity concentrations of re-melted glass matrix with 5 wt % loading levels old and new sample made without, and with pre-heat treatment at 150°C for 12 hr. under dynamic vacuum. Both samples were ~ 1.5 (±0.6) mm thick.

Fe^{2+}-doped fiber.

ChG-Fe:ZnSe matrix preforms with 0.5 wt% Fe and 1 wt% Fe were sent to the University of Nottingham for fiber drawing. Fibers 250 μm in diameter were drawn. Cleaved faces of drawn fibers are shown in Figure 16. The top row (0.5 wt%) shows less bubbles than the bottom row (1 wt%). We also note that bubbles are < 20 μm in diameter, an order of magnitude smaller than they were in the preform (Figure 17).

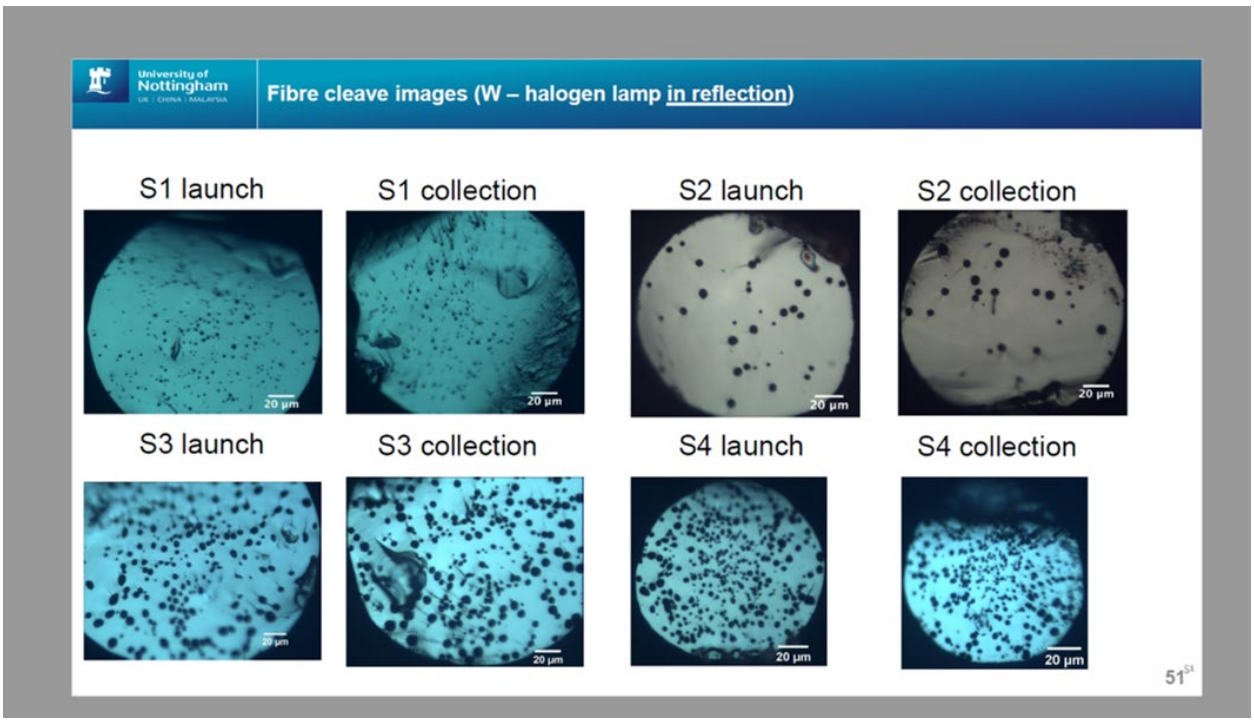

Figure 16. Fe^{2+}-doped ChG-ZnSe matrix drawn fibers. Fiber faces are shown after cleaving. S1 and S2 are 0.5 wt% Fe^{2}. S3 and S4 were 1 wt% Fe^{2}. Launch and collection refer to different ends of the fiber.

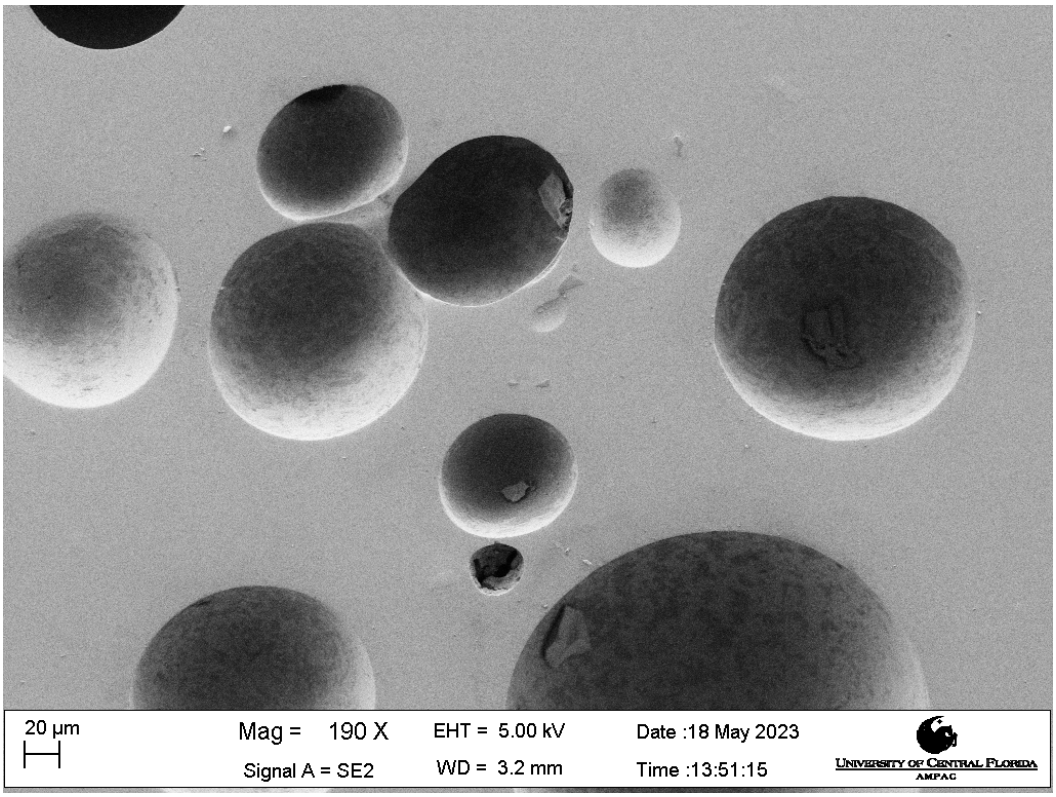

Figure 17. SEM image of composite preform bubble.

Fiber Fe^{2+} emission

The emission setup was revised to measure Fe^{2+} emission in the fibers. This consisted of fabricating a groove to hold the fiber in place in the cryostat. It also involved using a lens to focus the pump beam at the tip of the fiber. The fiber surface was angled relative to the pump beam at ~45°. Collection optics were set up to collect emission normal to the same fiber tip face. In spite of a valiant attempt, no Fe^{2+} emission was observed.

One issue with testing emissions from fiber samples is that the small facet size (~250 µm) makes alignment difficult, especially when the sample is held in a cryostat. To counteract this issue, emissions testing of bulk samples from the fiber preforms was proposed. Because the preforms are much larger in diameter than the fibers, alignment is simplified. In theory, illuminating the same area of the bulk samples should produce similar emissions as the fiber samples. Therefore, searching for emissions signal from bulk material under focusing conditions proposed for fiber emissions measurements should provide an estimate for the signal shape and amplitude expected during these more difficult measurements.

Initially, no emission was visible when illuminating the bulk sample with 1 mJ pulses at 125 µm focus. Previous measurements were performed with much higher pulse energies (~49 mJ) and larger spot sizes. During these measurements, damage was observed when 3 mJ pulses were focused to 125 µm. As such, increasing the pulse energy beyond 2 mJ is not possible. To increase the pulse energy, the beam was defocused to increase the spot size to 600 µm. The spot size was measured via knife edge scan by scanning between the 90% and 50% power transmission points. When the pulse energy was increased to 3.7 mJ, this yielded measurable emissions. Thus, our current detection setup (collection optics and detector sensitivity) was found to not be capable of sensing Fe^{2+} emission from a fiber tip due to damage limitations. A pump

laser with shorter pulse width but the same energy per pulse would give us a much better chance of observing Fe^{2+} emission without damaging the fiber tip. Also, reduction in fiber loss at emission wavelengths would provide stronger emission.

Facts:

- Uncoated ZnSe particles are dissolved at high melt temperatures in all multi-component chalcogenide glasses examined.
- We found that multicomponent ZnSSe forms when ZnSe particles are placed in an As_2Se_3-As_2S_3 glass melt.
- Thin alumina coatings deposited via ALD on ZnSe and Fe:ZnSe particles prevent dissolution into the chalcogenide glass when heating to modest melting temperatures for short times whereby ZnSe particles remain intact with minimal ZnS formation.
- Particle agglomeration during ALD was observed in early tests but improved processing has reduced that issue. The extent of agglomeration has been directly correlated to the moisture content present and has been reduced through an in-situ ozone treatment process. Further reduction in moisture levels has been realized by heat treating particles at all stages.
- Fe^{2+} emission was observed when laser pumping the solidified bulk composite glass-particle mixture.
- BG-Fe:ZnSe particle composite material was drawn into fiber but bubbles, agglomerates and moisture-related impurities remain in the fiber, preventing demonstration of lasing.

Program Management

Research Team

Our research team consisted of laser and optical materials experts from CREOL, The College of Optics & Photonics at the University Central Florida (UCF). Dr Kenneth L Schepler led the team as Principal Investigator. Dr Kathleen Richardson and Dr Martin Richardson served as Co-Principal Investigators. Dr Kathleen Richardson plus Dr Matthieu Chazot, Dr Rashi Sharma and Mr Alex Kostogiannes were responsible for fabricating the chalcogenide glass and Fe-doped ZnSe particle matrix. As of Fall 2021, Dr. Chazot departed the group for a new position in France. Dr. Rashi Sharma has assumed his role in the effort. Dr Kathleen Richardson was also responsible for physically characterizing bulk and fiber glass/ZnSe composite samples and compiling physical and optical characteristic data as a function of dopant loading level.

Dr Schepler was responsible for optically characterizing composite samples (scattering, absorption, emission, lifetime) and demonstrating lasing of bulk and fiber samples. Dr Martin Richardson provided the laser pumping and optical characterization facilities. Half/time graduate student (now Dr Justin Cook) co-advised by Dr Schepler and Dr Richardson assembled the laboratory setups and performed the optical measurements. Dr Cook passed along his knowledge to graduate student James Drake who completed optical measurements for this effort. Almost daily interaction between the materials and optics groups occurred to provide feedback on sample availability and sample characterization. We also conferred frequently with colleagues from AFRL, particularly colleagues from AFRL/RYDH (via CRADA) who have extensive experience with Fe:ZnSe and Cr:ZnSe laser assembly and testing. We provided bulk and fiber samples to AFRL/RYDH for testing throughout the program effort. They also provided us with HIP-ed Fe:ZnSe samples.

Dr Parag Banerjee at the College of Materials Science and Engineering (UCF) and his students have played a key role in our technical progress. His Atomic Layer Deposition capabilities [7] are unique and were key

to fabricating Fe-doped ZnSe particles that remain stable in a heated chalcogenide glass matrix. Initial runs performed last year were promising although there were issues with partial coating of some particles and tendencies for particle aggregation. He has made improvements to the ALD instrumentation as well as the process to provide fully coated ZnSe particles with much less particle aggregation.

Fiber drawing was successfully carried out by the group of Prof. Angela Seddon at University of Nottingham, UK. She has extensive experience in the fabrication of doped chalcogenide fibers for a variety of sensing applications, as evident in her recently concluded multi-year program as part of the European Horizon 2020 program [8] as well as over 38 publications in the past 5 years in the areas of mid-IR fiber lasers and sensors. Her activities were supported by the UCF team and by EOARD funds.

The program supported numerous graduate and undergraduate students throughout the program as evident in the co-author listing associated with the resulting publications below.

Covid-19

Covid-19 safety measures had a serious effect on our rate of progress during the 2020-2022 years of the effort. In-person meetings at UCF and travel to our collaborators in France and the United Kingdom were highly restricted. Even research in our labs were restricted and even stopped for several weeks. Thankfully, on-line meetings allowed us to continue our work but at a slower pace. Due to these issues, we requested and received approval of time extensions from 14 April 2022 to 14 April 2023.

Publications resulting from this work

Matthieu Chazot, Chanelle Arias, Myungkoo Kang, Cesar Blanco, Alexandros Kostogiannes, Justin Cook, Anupama Yadav, Vincent Rodriguez, Frederic Adamietz, Dominique Verreault, Sylvain Danto, Thomas Loretz, Angela Seddon, David Furniss, Kenneth Schepler, Martin C. Richardson, and Kathleen A. Richardson, "Investigation of ZnSe stability and dissolution behavior in As-S-Se chalcogenide glasses," Journal of Non-Crystalline Solids **555**, 120619 (2021).

Matthieu Chazot, Alexandros Kostogiannes, Matthew Julian, Corbin Feit, Jaynlynn Sosa, Myungkoo Kang, Cesar Blanco, Justin Cook, Vincent Rodriguez, Frederic Adamietz, Dominique Verreault, Parag Banerjee, Kenneth Schepler, Martin C. Richardson, and Kathleen A. Richardson, "Enhancement of ZnSe stability during optical composite processing via atomic layer deposition," Journal of Non-Crystalline Solids **576**, 121259 (2022).

Justin Cook, Matthieu Chazot, Alexandros Kostogiannes, Rashi Sharma, Corbin Feit, Jaynlynn Sosa, Parag Banerjee, Martin Richardson, Kathleen Richardson, and Kenneth L Schepler, "Optically active Fe^{2+}-doped ZnSe particles in a chalcogenide glass matrix " Optical Materials Express **12**, 1555-1563 (2022).

Corbin Feit, Jaynlynn Sosa, Alexandros Kostogiannes, Matthieu Chazot, Nicholas G. Rudawski, Titel Jurca, Kathleen A. Richardson, and Parag Banerjee, "Surface oxidation of hydrophobic ZnSe for enhanced growth of atomic layer deposited aluminum oxide," Journal of Vacuum Science & Technology A **40** (2022).

Alexandros Kostogiannes, Rashi Sharma, Andrew Howe, Matthieu Chazot, Myungkoo Kang, Justin Cook, Kenneth Schepler, and Kathleen A. Richardson, "Role of powder handling on resulting impurities in ZnSe-doped As-S-Se composite materials," Optical Materials Express **12**, 4287-4298 (2022).

Rashi Sharma, Alexandros Kostogiannes, Daniel Wiedman, Jaynlynn Sosa, Justin Cook, James Drake, David Furniss, Boyu Xiao, Angela Seddon, Parag Banerjee, Kenneth Schepler, and Kathleen Richardson, "Luminescent Fe:ZnSe doped As-S-Se optical composites for the mid-infrared," (SPIE, 2023, **12518**).

References

1. A. Sincore, J. Cook, F. Tan, A. El Halawany, A. Riggins, S. Mcdaniel, G. Cook, D. V. Martyshkin, V. V. Fedorov, S. B. Mirov, L. Shah, A. F. Abouraddy, M. C. Richardson, and K. L. Schepler, "High power single-mode delivery of mid-infrared sources through chalcogenide fiber," Optics Express **26**, 7313-7323 (2018).
2. Matthieu Chazot, Chanelle Arias, Myungkoo Kang, Cesar Blanco, Alexandros Kostogiannes, Justin Cook, Anupama Yadav, Vincent Rodriguez, Frederic Adamietz, Dominique Verreault, Sylvain Danto, Thomas Loretz, Angela Seddon, David Furniss, Kenneth Schepler, Martin C. Richardson, and Kathleen A. Richardson, "Investigation of ZnSe stability and dissolution behavior in As-S-Se chalcogenide glasses," Journal of Non-Crystalline Solids **555**, 120619 (2021).
3. Matthieu Chazot, Alexandros Kostogiannes, Matthew Julian, Corbin Feit, Jaynlynn Sosa, Myungkoo Kang, Cesar Blanco, Justin Cook, Vincent Rodriguez, Frederic Adamietz, Dominique Verreault, Parag Banerjee, Kenneth Schepler, Martin C. Richardson, and Kathleen A. Richardson, "Enhancement of ZnSe stability during optical composite processing via atomic layer deposition," Journal of Non-Crystalline Solids **576**, 121259 (2022).
4. Matthieu Chazot, "Verres chalcogénures dopés aux ions ferreux," in *Chemistry* (University of Laval, 2015), p. 116.
5. Justin Cook, Matthieu Chazot, Alexandros Kostogiannes, Rashi Sharma, Corbin Feit, Jaynlynn Sosa, Parag Banerjee, Martin Richardson, Kathleen Richardson, and Kenneth L Schepler, "Optically active Fe^{2+}-doped ZnSe particles in a chalcogenide glass matrix " Optical Materials Express **12**, 1555-1563 (2022).
6. NoSoung Myoung, Vladimir V. Fedorov, Sergey B. Mirov, and Lowell E. Wenger, "Temperature and concentration quenching of mid-IR photoluminescence in iron doped ZnSe and ZnS laser crystals," J. Lumin. **132**, 600-606 (2012).
7. Zhengning Gao, and Parag Banerjee, "Review Article: Atomic layer deposition of doped ZnO films," Journal of Vacuum Science & Technology A **37**, 050802 (2019).
8. A. B. Seddon, "The Minerva Project," https://www.nottingham.ac.uk/research/groups/ggiemr/research/projects/the-minerva-project.aspx.